PERGAMON

International Journal of Solids and Structures 36 (1999) 4919–4940

INTERNATIONAL JOURNAL OF SOLIDS and STRUCTURES

Two-dimensional discrete element simulations of ice–structure interaction

A.P.S. Selvadurai*, K. Sepehr

Department of Civil Engineering and Applied Mechanics, McGill University, Montreal, Que., Canada H3A 2K6

Received 1 May 1998; accepted 10 August 1998

Abstract

The paper presents the application of a discrete element technique for the study of the plane strain problem of the interaction between a moving ice sheet and a flexible stationary structure. The discrete element technique accounts for the generation of failure within an initially intact ice sheet. The failure of the ice corresponds to situations where the ice can exhibit combinations of brittle fragmentation and viscoplastic flow. The modelling also accounts for size dependency in the strength of the ice after fragmentation. The inter-fragment interactions are modelled by non-linear constraints which includes Coulomb frictional behaviour. The computational scheme is used to evaluate the time history of the average contact stresses and the distribution of local contact stresses at the ice–structure interface in the fragmentation zone.

Keywords: Ice–structure interaction; Discrete element technique; Ice fragmentation; Ice mechanics; Size effects in fragmentation; Computational ice mechanics

1. Introduction

The dynamic interaction between a moving ice sheet and a stationary structure is a very complex process which is governed by a number of factors including the constitutive behaviour of the ice, the configuration and flexibility of the structure, the contact conditions at the ice–structure interface, the speed of movement of the ice sheet and spatial distributions of the geometric features of an ice sheet which can include pressure ridges, brine inclusions and other inhomogeneities and the evolutionary history of the ice sheet. The consideration of all the above factors in a dynamic ice–structure interaction scenario is a difficult exercise. As a result, the modelling of an ice–structure interaction had evolved along several distinct lines. In the most elementary of these treatments, the ice–structure system is represented by analogue models (e.g. Matlock et al., 1971; Eranti et al., 1981; Sodhi and Nakazawa, 1990; Eranti, 1992). The elements of analogues or the analogue models

* Corresponding author. Fax: 001 514 398 7361; e-mail: apss@civil.lan.mcgill.ca

0020-7683/99/$ - see front matter
PII: S0020-7683(98)00272-8

can include springs, dashpots, non-linear friction elements and masses to represent the various aspects of the mechanical and physical variables in the interaction problem. These representations, although convenient from the point of view of computations, lack the degree of uniqueness necessary to accurately define parameters associated with the modelling. Furthermore, these elementary models are not altogether versatile in representing the specific processes associated with ice failure and ridge-build up processes which are characteristic features of the persistent interaction of moving ice sheets and stationary structures. An improvement to these analogue models focuses on the continuum representation of the mechanical behaviour of ice. Such continuum modelling has attracted a great deal of attention over the past two decades, especially in relation to the modelling of ice behaviour by appeal to continuum representations of elastic, plastic, creep, damage and viscoplastic phenomena (e.g. Jellinek, 1958; Croasdale, 1984; Timco and Frederking, 1984; Nadreau and Michel, 1986; Hallam and Pickering, 1988; Blanchet, 1988; Karr and Choi, 1989; Joensuu and Riska, 1989; Jordaan and McKenna, 1989; Selvadurai and Au, 1992; Comfort et al., 1992; Jordaan and Xiao, 1992; Buck et al., 1994; Nixon et al., 1994; Selvadurai and Sepehr, 1995). These continuum representations of ice behaviour have in turn been used to examine the ice–structure interaction process. A major drawback in the use of continuum descriptions of ice behaviour is that the interaction takes place with the development of separate elastic, plastic, damage, creep and viscoplastic zones which individually maintain their continuum character. This is very much at variance with the observations of full scale interactions between moving ice sheets and stationary structures where the ice sheet experiences fragmentation and progressive fragmentation during the persistent movement of an ice sheet against a structure (see e.g. Jefferies and Wright, 1988; Sanderson, 1988). These processes are invariably absent in all constitutive responses governed by continuum descriptions.

The continuum models, even when extended to include large strain phenomena or even localization phenomena, will not adequately model brittle fragmentation, crushing and large scale movement of the ice fragments in the interaction zones. The ability to model an ice sheet which can accommodate a transition from an initially intact state to a fragmented transformed state is recognized as an essential step towards a realistic simulation of the dynamic ice–structure interaction process. A method of accommodating such a process is to consider the fragmentation of the ice sheet during the interaction process. Although the initiation and evolution of fragmentation can be examined by utilizing computational methodologies based on finite element and boundary element schemes (e.g., Ingraffea and Saouma, 1984; Ingraffea, 1987; Selvadurai et al., 1993; Selvadurai, 1995; Selvadurai and ten Busschen, 1995), these developments have not advanced to the point where the processes associated with fragment separation, large scale fragment movement, fragment interaction during large scale movement, etc., can be examined without considerable further research.

The capabilities for modelling fragment initiation from an initially continuum state, large scale fragment movement and the continued evolution of fragments are regarded as essential ingredients for the successful modelling of processes which are observed in the vicinity of the ice–structure interaction zone. The application of discrete element modelling techniques to the study of ice–structure interaction is therefore considered a useful methodology which can address the deficiencies associated with some of the methodologies proposed in the literature in ice–structures interaction. Some earlier applications of discrete element techniques to the study of ice–structure interaction are due to Hocking et al. (1985a, b, 1987), Williams et al. (1986) and Mustoe et al.

(1987) who have examined the interaction of planar ice sheets with stationary structures. The discrete element procedures developed by these authors have the facility to accommodate a transition from a continuum to a fragmented state through the application of relatively simple criteria. In addition, the large scale movements and interactions of ice fragments are accommodated through considerations of the dynamics of the fragments to which non-linear interactive constraints can be assigned.

In this study the basic concepts and methodologies advocated in discrete element modelling procedures are extended to examine the dynamic ice–structure interaction process. The first modification relates to the introduction of the concept of viscoplastic failure in regions where the state of stress is predominantly compressive and brittle fragmentation in regions where the stress state is predominantly tensile. Experimental observations tend to support such processes. The second aspect of the research introduces the concept of a size-dependent fragmentation stress. Such size dependency is regarded as a characteristic feature in the fragment development in most brittle geomaterials (e.g., Jahns, 1966; Bieniawski, 1968; Pratt et al., 1972).

The present paper applies a discrete element procedure which includes viscoplasticity and size dependency effects to the study of the interaction between a flexible stationary structure and an ice sheet of constant thickness which impacts the structure with a specified velocity. The results of the computational modelling illustrate the fragment development from an originally intact ice, the fragment movement and continued fragmentation in regions of the fragmented ice mass. The time history of the average contact stresses and the distribution of local contact stresses developed at the ice–structure contact zone are also presented.

2. Constitutive modelling

The discrete element modelling of the ice–structure interaction process takes into consideration the following constitutive responses: (i) the constitutive behaviour of the intact ice mass; (ii) the criteria for the initiation of fragmentation; (iii) the responses characterizing interaction between fragments; and (iv) the deformability or flexural characteristics of the structure.

2.1. Constitutive behaviour of the intact ice

Intact ice can exhibit a variety of constitutive responses depending upon its origin. Ice is a strongly heterogeneous and anisotropic material, the constitutive behaviour of which can be described by elastic, viscoelastic, creep, damage and viscoplastic components of mechanical response. Although the polycrystalline nature of ice in the granular scale contributes to the anisotropic effects, in the current study, the constitutive behaviour of the ice is modelled by an isotropic elastic–viscoplastic model.

2.2. Elastic behaviour

The rate form of the isotropic elastic constitutive model is given by

$$\dot{\varepsilon}^{e}_{ij} = \frac{\dot{\sigma}'_{ij}}{2G} + \frac{\dot{\sigma}_{kk}}{9K}\delta_{ij} \tag{1}$$

where $(\dot{})$ denotes the time derivative, $\dot{\sigma}'_{ij}$ is the stress deviator rate and G and K are, respectively, the linear elastic shear modulus and the bulk modulus.

2.3. Viscoplastic behaviour

The viscoplastic model for ice, represents material behaviour that is governed by yield criteria in which time-dependent plastic deformation takes place if stress states associated with these yield criteria are attained. Viscoplastic flow can continue for all stress states which satisfy the yield criteria. The viscoplasticity model proposed by Perzyna (1966) has been successfully applied by a number of investigators, including Zienkiewicz and Cormeau (1974), Cormeau (1975) and Selvadurai and Au (1992) for the computational modelling of a variety of geomaterials. The viscoplastic strain rate is given by

$$\dot{\varepsilon}_{ij}^{\mathrm{vp}} = \gamma \langle \Phi(F) \rangle \frac{\partial F}{\partial \sigma_{ij}} \tag{2}$$

where γ is a fluidity parameter, F is the current yield function and $\Phi(F)$ is a flow function defined by

$$\begin{aligned} &\langle \Phi(F) \rangle = \Phi(F); \quad \text{if } F \geqslant 0 \\ &\langle \Phi(F) \rangle = 0; \quad \text{if } F < 0 \end{aligned} \tag{3}$$

The flow function $\Phi(F)$ is a material property which needs to be determined through experiments. Two commonly used representations, however, are

$$\Phi(F) = \exp\{M(F-F_0)/F_0\} - 1 \tag{4}$$

and

$$\Phi(F) = \{(F-F_0)/F_0\}^N \tag{5}$$

where M and N are constants and F_0 is a uniaxial failure stress.

Similarly, the yield function F needs to be determined by recourse to experiments. In this study, however, attention is restricted to the Mohr–Coulomb yield function where

$$F = \frac{I_1}{3}\sin\phi + \sqrt{J_2}\left\{\cos\Theta - \left(\frac{1}{\sqrt{3}}\right)\sin\Theta\sin\phi\right\} - c\cos\phi \tag{6}$$

where

$$\begin{aligned} &I_1 = \sigma_{kk}; \quad J_2 = \tfrac{1}{2}\sigma'_{ij}\sigma'_{ij}; \quad J_3 = \tfrac{1}{3}\sigma'_{ij}\sigma'_{jk}\sigma'_{ki} \\ &\Theta = \tfrac{1}{3}\sin^{-1}\{-(3\sqrt{3}J_3)/(2J_2^{3/2})\}; \quad (-\pi/6 \leqslant \Theta \leqslant \pi/6) \\ &\phi = \text{angle of internal friction}; \quad c = \text{cohesion} \end{aligned} \tag{7}$$

The yield behaviour in the tension range is truncated by incorporating a tension cut-off σ_{T}. In this case the Mohr–Coulomb yield criterion is a three parameter model which is defined by c, ϕ and σ_{T}.

2.4. Initiation of fragmentation

Fragmentation, as opposed to yielding, involves the process of breakage of intact ice. The mode of fragment development is largely dependent on the state of stress within an intact ice region. It is reasonable to assume that states of stress in which the tensile stresses dominate are more susceptible to fragment development. In an intact ice region, processes which initiate fragment development are directly related to the strength parameters associated with the attainment of peak strength. The principal stresses and their orientations within each element can be evaluated during the stress analysis procedure. The attainment of either a critical compressive strength or a tensile strength can be assumed for the initiation of fragment development.

2.5. Fragment initiation in compression

The process of fragment development during compressive shear failure is prescribed by considering the Mohr–Coulomb criterion. This criterion can be written in terms of the principal stresses in the form

$$\sigma_1 \geqslant \sigma_c + \sigma_3 \tan^2 (45 + \phi/2) \tag{8}$$

where σ_c is the unconfined strength in compression, ϕ is the angle of internal friction and σ_1 and σ_3 are, respectively, the maximum and minimum principal stresses. The unconfined compressive strength σ_c is related to the shear strength parameters c and ϕ associated with the Mohr–Coulomb failure criterion according to

$$\sigma_c = 2c\{(\tan^2 \phi + 1)^{1/2} + \tan \phi\} \tag{9}$$

For the compression failure mode there are two possible conjugate orientations of fragmentation inclined at equal angles $(\pi/2 - \phi/2)$ to the direction of the stress on either side of it. In two dimensions, these are defined by

$$\theta = \tan^{-1} \left\{ \frac{(\sigma_1 - \sigma_{xx})}{\sigma_{xy}} \right\} \pm \left(\frac{\pi}{4} - \frac{\phi}{2} \right) \tag{10}$$

where θ is the angle between the fragmentation plane and the positive global axis, σ_{xx} is the x-component of the stress tensor and σ_{xy} is the shear component of the stress tensor. In the computational modelling, the sign of the second term on the right-hand-side of (10) is determined by using a random number generator. This allows for the development of a relatively random fragmentation pattern as a series of elements experience fragmentation.

2.6. Fragment initiation in tension

The tensile fragmentation criterion assumes that the material will fragment when the minimum principal stress σ_3 reaches the tensile strength of the material, σ_T (note that the tensile stresses are considered negative). For two dimensions, the criterion can be written as

$$\sigma_3 \geqslant \sigma_T \tag{11}$$

The orientation of the fragmentation plane is given by

$$\theta = \tan^{-1}\left\{\frac{\sigma_1 - \sigma_{xx}}{\sigma_{xy}}\right\} \tag{12}$$

where θ is the angle between the fragmentation plane and the positive global x-axis. In this case, the θ-direction is aligned with the maximum principal stress direction. This type of modelling attempts to account for the limits to the tensile yield region in the ice which manifests as a result of defects within the material. The methodology originates from rock mechanics applications (e.g., Jaeger, 1967; Hobbs, 1967; Jaeger and Cook, 1976; Goodman, 1980) and the tensile zone failure is limited by brittle fragmentation. If tensile fragmentation is to occur in a region which has experienced viscoplastic flow in compression and post peak softening, the value of σ_T is replaced by its residual value, σ_{Tr}.

2.7. Viscoplastic flow vs fragmentation

In the previous section we have described the separate processes and criteria which govern the initiation of either viscoplastic flow or fragment development in the intact ice. During the ice–structure interaction process, both processes can occur within various regions of the ice sheet. From the computational point of view, the criterion which initiates fragmentation [eqns (8) and (11)], could be structured to initiate either process. Experimental observations on both ice and other geomaterials (Jaeger and Cook, 1976; Sanderson, 1988), however, tend to support the postulate that the processes of brittle fragmentation would occur in regions where the stress state is predominantly tensile and viscoplastic flow would occur in regions where the state of stress is predominantly compressive. Such an assumption would enable the utilization of the same failure criteria for describing both the initiation of viscoplastic flow in the compression range and fragmentation in the tensile range. The consideration of distinct stress states which will initiate either viscoplastic flow or fragment development can be ascertained only by appeal to experimentation. In this study, fragment development and failure initiation for viscoplastic flow are described by the Mohr–Coulomb criterion specified in terms of c and ϕ. In the computational schemes two types of responses of the ice are adopted; these are described in the following:

(i) In the first model, it is assumed that the intact ice will experience brittle fragmentation in both tensile and compressive modes for all choices of σ_1 and σ_3;
(ii) In the second model it is assumed that the intact ice will experience brittle fragmentation only for situations where either a single principal stress component or both are in the tensile mode and viscoplastic flow will occur only for stress states involving purely compressive stress states for both principal stresses. In the case where viscoplastic flow occurs first, there is provision for subsequent brittle fragmentation in tension. This subsequent fragmentation will be governed by the prescribed strength characteristics of the ice.

2.8. Fragment interaction responses

The interaction between ice fragments is characterized by normal (n) and shear (s) interaction responses which relate the normal and shear inter-fragment forces to the respective differential displacements at the contacting surfaces. In general, these relationships can have non-linear responses characterized by elastic-non-linear irreversible phenomena (e.g. Selvadurai and Boulon,

1995). The simplest inter-fragment interactive response assumes that the incremental change in the contact force between two contacting planes is given by a stiffness relationship of the form

$$dF_i = k_j(du_i^1 - du_i^2) \tag{13}$$

where $i = n, s$ and dF_i are the incremental changes in the contact force per unit length between the contacting planes, du_i^1 and du_i^2 are displacement increments at the contact plane between regions (1) and (2) and k_j are stiffness coefficients defined in the normal and shear directions of the average plane of orientation at the point of contact. The stiffnesses themselves can be a function of the differential displacements $(du_i^1 - du_i^2)$. The simplest form of an inter-fragment contact response is defined by elastic stiffness values which can be derived from the theory of Hertzian contact between plane bodies. An elasto–plastic interface relationship can be constructed, particularly to account for the shear behaviour at the contact region between fragments. With material such as fragmented ice, the inter-fragment shear behaviour can exhibit a wide range of responses which could include dilatant friction, Coulomb friction and adhesion which will be temperature, rate and ice-type dependent. In this study, the generated inter-fragment shear behaviour is characterized by a Coulomb friction (μ_f) and an adhesion (c_f) based limiting value in the shear behaviour.

For this response,

$$k_s = k_s^*; \quad |d\tau_s| < c_f + \mu_f \sigma_n \tag{14}$$

$$k_s = 0; \quad |d\tau_s| = c_f + \mu_f \sigma_n \tag{15}$$

where μ_f is the coefficient of inter-fragment friction, c_f is the inter-fragment adhesion, τ_s is the inter-fragment shear and σ_n is the inter-fragment normal stress. The interaction response in the normal direction, is assumed to be elastic, provided the contact force between fragments is compressive. The interactive stiffness will vanish when the fragments separate, i.e.

$$k_n = k_n^*; \quad d\sigma_n \leqslant 0 \tag{16}$$

$$k_n = k_s = 0; \quad d\sigma_n > 0 \tag{17}$$

2.9. Size dependency of strength

Polycrystalline geomaterials, such as ice and rock, are composed of crystals and grains in a fabric that can include defects such as cracks and fissures. When the size of a specimen is small, such that only relatively few defects are present, failure is forced to involve new crack initiation and growth, whereas a material loaded through a larger volume will encounter pre-existing flaws at critical locations. Thus, the material strength can be size-dependent. In particular, brittle geomaterials such as coal, granitic rocks and shale exhibit the greatest degree of size dependency; the ratio of laboratory to field strengths sometimes attaining values in excess of 10. Some limited but definitive studies have been made to examine the influence of size effects on the strength over a broad range of specimen sizes. Bieniawski (1968) reported tests on prismatic in situ coal specimens measuring up to $1.6 \times 1.6 \times 1.0$ m. Results of tests conducted by Jahns (1966) on cubical specimens of calcareous iron ore and tests conducted by Pratt et al. (1972) on fissured quartz diorite also support the size-dependency hypothesis. Available data from these investigations are insufficient to provide a conclusive recommendation valid for a variety of polycrystalline materials; however,

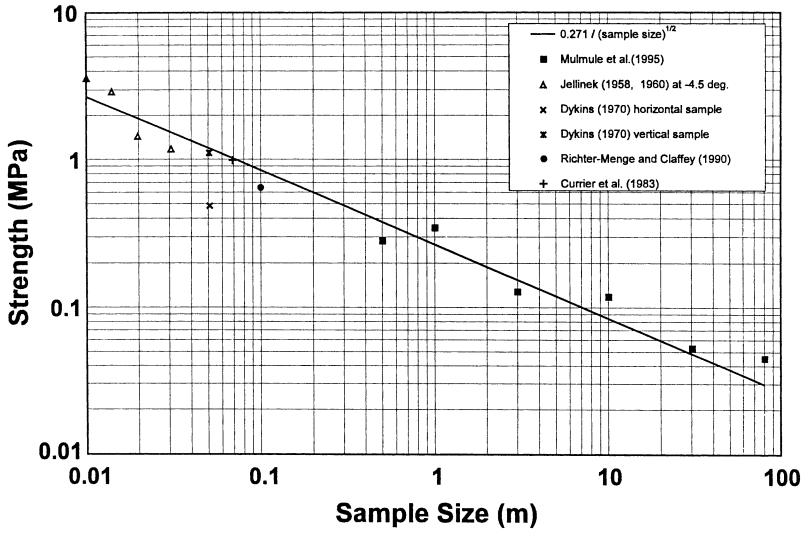

Fig. 1. Size dependency on the tensile and fracture strength of ice: experimental data.

these results generally indicate that there is a limiting size beyond which larger specimens exhibit no further decrease in strength. Figure 1 illustrates the relationship between the tensile strength of ice and the larger specimen edge length, which is derived from experimental results available in the literature (Fleet Technology, 1996). As is evident, the tensile strength of ice (σ_T) increases with progressively smaller specimen size confirming the size dependency of ice strength.

If size dependency (i.e. a form of size dependency relationship which leads to a significant increase in strength as the size of the fragment decreases) is not accounted for in the computational modelling, the fragmentation process can proceed indefinitely until the size of the fragments will result in the continual reduction of the time increments in the computational scheme necessary for its stability and convergence; this process will effectively terminate the computational procedure. The relationship shown in Fig. 1 is thus modified in order to limit the fragment size development. In these computational developments it is assumed that the tensile as well as the shear strength parameters of ice will increase exponentially (similar to the results on the rock specimens reported in the literature) as the specimen size falls below a certain edge length (in this study this edge length is limited to 0.2 m). The analysis, however, is not restricted to this value of the edge length. This particular value is adopted primarily to illustrate the processes involved and to examine the effectiveness of the approach. Given sufficient computing resources, this value can be further reduced. In the two-dimensional plane strain modelling, the edge length of a fragment is defined in relation to the diameter of a circle of equivalent area. The modified forms of the size dependency relationships are shown in Fig. 2(a) and (b). The imposed limitation is necessary in order to limit the excessive demand for computing time required to examine ice–structure interaction problems even with a relatively coarse initial descretization of the ice sheet configuration. The shear strength parameters of ice (c, ϕ), are, however, assumed to remain constant at a prescribed reduced specimen size since there is insufficient data to postulate a conclusive relationship for size dependency of ice in compression.

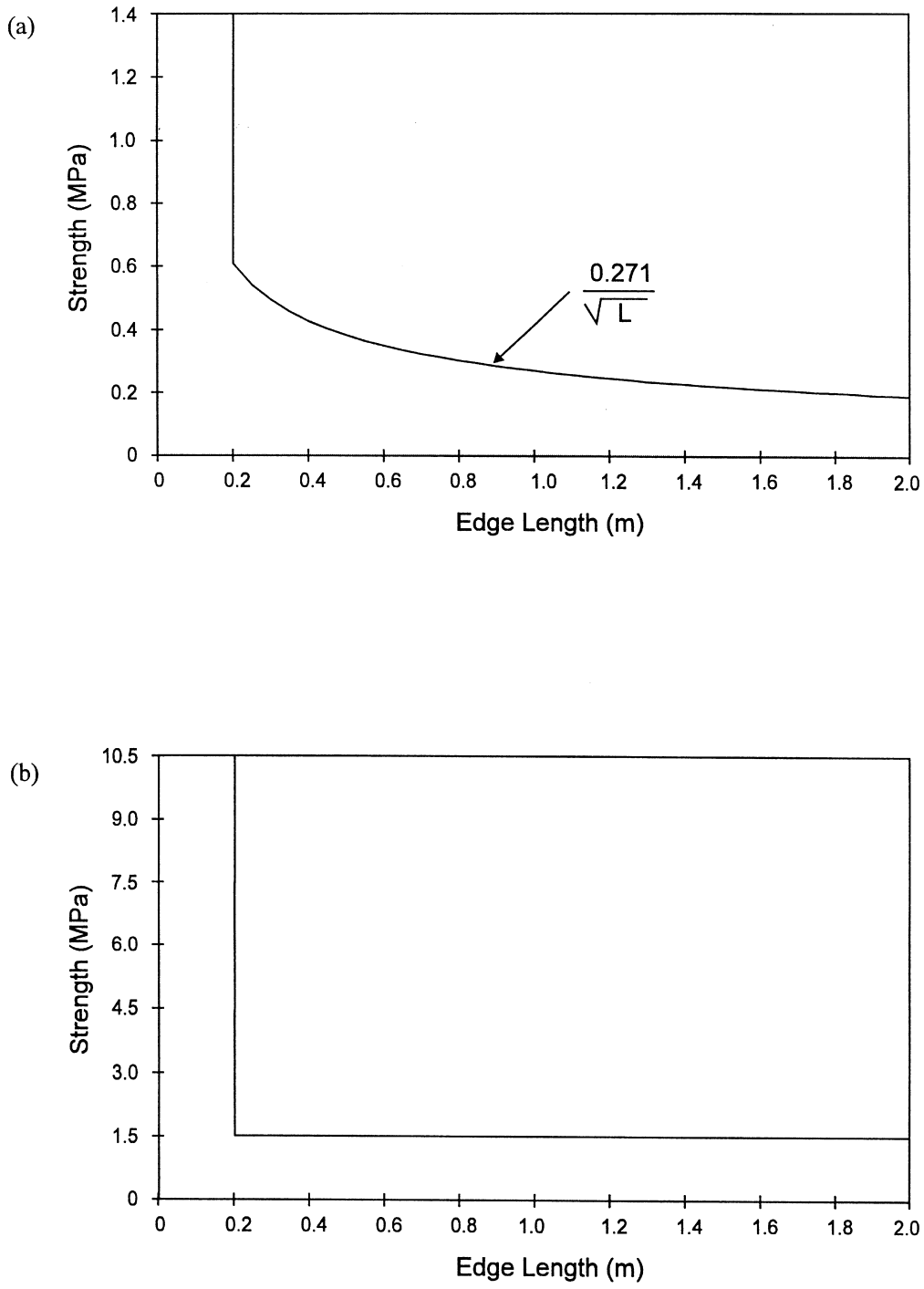

Fig. 2. Modified size dependency relationship for strength of ice: (a) Tensile strength; (b) compressive strength.

3. Computational aspects

The discrete element approach which includes a transformation of an initially continuum region to a fragmented state involves a sophisticated computational scheme which has many facets. There are two aspects of the computational scheme which merit further discussion, purely because these procedures have a bearing on the accuracy and efficiency of the solution algorithm. The principal computational aspects associated with the discrete element modelling of a fragmentable viscoplastic material basically involved two components: these are

(a) the procedures used to examine the non-linear material phenomena such as a viscoplasticity and non-linear inter-fragment interaction and
(b) the procedures used in the solution of the dynamic equations of motion associated with the entire system of interacting fragments, intact continuum regions and structural components.

3.1. Computational procedures for viscoplasticity

The computational procedures for viscoplasticity are well documented in a number of articles including those by Zienkiewicz and Cormeau (1974) and Owen and Hinton (1980). Briefly, the viscoplastic strain increment at time interval $\Delta t_n = (t_{n+1} - t_n)$ can be obtained via a scheme given by

$$(\Delta \boldsymbol{\varepsilon}^{\mathrm{vp}})_n = \Delta t_n \{(1-\Omega)(\dot{\boldsymbol{\varepsilon}}^{\mathrm{vp}})_n + \Omega(\dot{\boldsymbol{\varepsilon}}^{\mathrm{vp}})_{n+1}\} \tag{18}$$

where Ω takes the following value depending upon the integration scheme:

$$\Omega = 0, \text{fully explicit}; \quad \Omega = 1, \text{fully implicit}; \quad \Omega = 1/2, \text{Crank–Nicholson} \tag{19}$$

The incremental stress at the iteration n can be given in the form

$$(\Delta \boldsymbol{\sigma})_n = [\mathbf{D}^{-1} + \Omega(\Delta t_n)\mathbf{H}_n]^{-1}\{[\mathbf{B}]_n(\Delta \mathbf{d})_n - (\dot{\boldsymbol{\varepsilon}}^{\mathrm{vp}})_n(\Delta t_n)\} \tag{20}$$

where

$$(\Delta \boldsymbol{\varepsilon})_n = [\mathbf{B}]_n(\Delta \mathbf{d})_n \tag{21}$$

$$(\Delta \boldsymbol{\varepsilon}^{\mathrm{vp}})_n = (\dot{\boldsymbol{\varepsilon}}^{\mathrm{vp}})_n(\Delta t_n) - \{\Omega(\Delta t_n)(\mathbf{H})_n\}(\Delta \boldsymbol{\sigma})_n \tag{22}$$

$$(\mathbf{H})_n = \left(\frac{\partial \dot{\boldsymbol{\varepsilon}}^{\mathrm{vp}}}{\partial \boldsymbol{\sigma}}\right)_n \tag{23}$$

and $\mathbf{D}$ is the elasticity matrix given by

$$\dot{\boldsymbol{\sigma}} = \mathbf{D}\dot{\boldsymbol{\varepsilon}}^{\mathrm{e}} \tag{24}$$

During a time increment (Δt_n), the incremental equation of equilibrium to be satisfied at any time t_n, take the integral form

$$\int_v [\mathbf{B}]_n^{\mathrm{T}}(\Delta \boldsymbol{\sigma})_n \, \mathrm{d}v + (\Delta \mathbf{f})_n = 0 \tag{25}$$

where $(\Delta\mathbf{f})_n$ is the vector of applied incremental forces during (Δt_n). The incremental displacement occurring during time increment (Δt_n) can be obtained in the form

$$(\Delta\mathbf{d})_n = [\mathbf{K}_T]_n^{-1} \int_v [\mathbf{B}]_n^T [\mathbf{D}^{-1} + (\mathbf{C})_n]^{-1} (\dot{\boldsymbol{\varepsilon}}^{vp})_n (\Delta t_n) \mathbf{dv} + (\Delta\mathbf{f})_n \tag{26}$$

and

$$[\mathbf{K}_T]_n = \int_v [\mathbf{B}]_n^T [\mathbf{D}^{-1} + (\mathbf{C})_n]^{-1} [\mathbf{B}]_n \, dv \tag{27a}$$

where

$$(\mathbf{C})_n = \Omega(\Delta t)_n (\mathbf{H})_n \tag{27b}$$

The displacement increments, back substituted into (20) gives the stress increments $(\Delta\boldsymbol{\sigma})_n$:

$$(\Delta\boldsymbol{\sigma})_n = \mathbf{D}[\mathbf{B}(\Delta\mathbf{d})_n - (\dot{\boldsymbol{\varepsilon}}^{vp})_n (\Delta t)_n] \tag{28}$$

Also,

$$\begin{aligned} (\boldsymbol{\sigma})_{n+1} &= (\boldsymbol{\sigma})_n + (\Delta\boldsymbol{\sigma})_n \\ (\mathbf{d})_{n+1} &= (\mathbf{d})_n + (\Delta\mathbf{d})_n \\ (\boldsymbol{\varepsilon}^{vp})_{n+1} &= (\boldsymbol{\varepsilon}^{vp})_n + (\Delta\boldsymbol{\varepsilon}^{vp})_n \end{aligned} \tag{29}$$

The evaluated stress increment $(\Delta\boldsymbol{\sigma})_n$ is based on a linearized version of the equilibrium equations in integral form. Hence, the total stresses given by $(\boldsymbol{\sigma})$ will not exactly satisfy the complete equations of equilibrium. The incorporation of an out-of-balance or residual force Ψ in each cycle will minimize the error, i.e.

$$(\Psi)_{n+1} = \int_v [\mathbf{B}]_{n+1}^T (\boldsymbol{\sigma})_{n+1} \, dv + (\mathbf{f})_{n+1} \neq 0 \tag{30}$$

This residual force is then added to the applied force increment at the subsequent step.

The time integration scheme is unconditionally stable if $\Omega \geqslant 1/2$; i.e. the procedure is numerically stable but does not ensure accuracy of the solution. Consequently, even for values of $\Omega \geqslant 1/2$, limits must be imposed on the selection of the time step to achieve a valid solution. For viscoplasticity problems which are based on an associative flow rule ($Q = F$); a linear flow function for $\Phi(F) = F$ and if F is described by the Mohr–Coulomb yield criterion, the recommended limit (see e.g. Zienkiewicz and Cormeau, 1974) for the time increment is

$$\Delta t \leqslant \frac{4(1-\nu)(1-2\nu)F_0}{\gamma(1-2\nu+\sin^2\phi)E} \tag{31}$$

where F_0 is the equivalent uniaxial yield stress ($c\cos\phi$) and E is Young's modulus.

The solution algorithm for viscoplastic materials experiencing dynamic effects is fully described in the literature in computational mechanics. The change in the displacement associated with the viscoplastic strain is

$$\Delta\mathbf{d} = \mathbf{K}^{-1}\{\int(\mathbf{B}^{\mathrm{T}}\mathbf{D}\,\mathrm{d}\boldsymbol{\varepsilon}^{\mathrm{vp}}\Delta V + \Delta\mathbf{f}\} \tag{32}$$

where $\Delta\mathbf{f}$ represents the change in load during the time interval $\Delta\mathbf{t}$. The resulting stress change is

$$\Delta\boldsymbol{\sigma} = \mathbf{D}(\mathbf{B}\Delta\mathbf{d} - \Delta\mathbf{t}\,\mathrm{d}\boldsymbol{\varepsilon}^{\mathrm{vp}}) \tag{33}$$

The updated stress matrix after the increment of time $\Delta\mathbf{t}$ is

$$\boldsymbol{\sigma}^{(1)} = \boldsymbol{\sigma}^{(*)} + \Delta\boldsymbol{\sigma} \tag{34}$$

where $\boldsymbol{\sigma}^{(*)}$ is the initial stress matrix. After n time steps, the stress state is given by

$$\boldsymbol{\sigma}^{(n+1)} = \boldsymbol{\sigma}^{(n)} + \Delta\boldsymbol{\sigma}^{(n)} \tag{35}$$

These procedures are standard (Owen and Hinton, 1980) where $\Delta\boldsymbol{\varepsilon}$ is treated as in the method of initial strains. The procedure can be continued until the required duration of the simulation is achieved.

3.2. Computational procedures for the discrete element method

The basic concept of the discrete element method involves the solution of the dynamic equations of equilibrium for the intact continuum and for all fragments in the system. For each discrete element, the dynamic equilibrium equations can be written in the form

$$[\mathbf{M}]\left\{\frac{\mathrm{d}^2}{\mathrm{d}t^2}[\mathbf{u}]\right\} + [\mathbf{C}]\left\{\frac{\mathrm{d}}{\mathrm{d}t}[\mathbf{u}]\right\} + [\mathbf{K}]\{\mathbf{u}\} = \{\mathbf{f}\} \tag{36}$$

where $\{\mathbf{u}\}$ is the displacement; $\{\mathbf{f}\}$ is the force; $[\mathbf{M}]$, $[\mathbf{C}]$ and $[\mathbf{K}]$ are, respectively, mass, damping and stiffness matrices. The solution of the dynamic equations of equilibrium is constrained by: (i) incrementally non-linear material phenomena occurring within the non-linear regions; (ii) non-linear interactive phenomena at the boundaries of fragments; (iii) non-linear constraints concerning contact/separation at fragment boundaries; and (iv) non-linear constraints concerning fragment evolution.

The algorithms for the solution of the equations take advantage of a modal decomposition approach which presents certain advantages in the explicit formulation of the discretized forms of the governing equations, i.e.

$$\left\{\frac{\mathrm{d}^2}{\mathrm{d}t^2}[\mathbf{u}]\right\}_n = [\mathbf{M}]^{-1}\left[\{\mathbf{f}\}_n - [\mathbf{C}]\left\{\frac{\mathrm{d}}{\mathrm{d}t}[\mathbf{u}]_{n-1/2} - [\mathbf{K}]\{\mathbf{u}\}_n\right\}\right] \tag{37}$$

and

$$\left\{\frac{\mathrm{d}}{\mathrm{d}t}[\mathbf{u}]\right\}_{n+1/2} = \left\{\frac{\mathrm{d}}{\mathrm{d}t}[\mathbf{u}]\right\}_{n-1/2} + \left\{\frac{\mathrm{d}^2}{\mathrm{d}t^2}[\mathbf{u}]\right\}_n (\Delta t) \tag{38}$$

$$\{\mathbf{u}\}_{n+1/2} = \{\mathbf{u}\}_n + \left\{\frac{\mathrm{d}}{\mathrm{d}t}[\mathbf{u}]\right\}_{n+1/2} (\Delta t) \tag{39}$$

where Δt is the time increment and the subscripts denote the time step number. In the explicit

algorithm, the equations of motion are integrated separately using an explicit central technique. The stability condition for the time increment Δt, which employs an explicit-explicit partition (applicable to linear systems), takes the form

$$\Delta t \leqslant 2\{(1+\tilde{D}^2)^{1/2} - \tilde{D}\}/\omega_{\max} \tag{40}$$

where $\omega_{\max}$ is the maximum frequency of the combined system involving both rigid body motion and deformability of the system; and $\tilde{D}$ is the fraction of critical damping at $\omega_{\max}$.

Other stability criteria have been proposed in the literature on computational methods for transient dynamic analysis; these include

$$\Delta t \leqslant 2/\omega_{\max} \tag{41}$$

and

$$\Delta t \leqslant \eta L \left(\frac{\rho(1+v)(1-2v)}{E(1-v)}\right)^{1/2} \tag{42}$$

where η is a coefficient which depends on the element type used and L is the smallest length between any two nodes. This constraint is found to be suitable for application to non-linear systems.

4. Ice–structure interaction modelling

We apply the discrete element method which incorporates the aspects described previously to examine the interaction between a stationary flexible structure and an ice sheet moving at a constant speed. The computations are conducted only for specific choices of the constitutive behaviour of the ice sheet which is governed by the viscoplastic and fragmentation responses.

4.1. Modelling of structural response

The stationary, flexible structure is a cantilever which has a height of 20 m and a width of 1.8 m. The structure is modelled by elastic beam bending elements which exhibit a state of plane strain. The structural properties are indicated in Table 1. The fluid–structure interaction aspects of the structural response are not accounted for in the discrete element analysis. The region of the structure initially in contact with the ice sheet and subsequently in contact with the ice fragments, is modelled by a thin layer of zero-tension material elements. This ensures that the contact between the ice and the structure is always unilateral and does not experience tensile tractions at any location of the contact region during the ice–structure interaction process. During compression, however, the interface will exhibit frictional characteristics which are assumed to be approximately equal to the ice–fragment contact responses. The structural parameters used in the modelling are given in Table 1.

4.2. Modelling of the ice sheet

The ice sheet is assumed to have a finite length of 65 m and a constant thickness of 2 m. In its initial state, the ice sheet is assumed to be isotropic in its constitutive responses. The constitutive

Table 1
Input data

Ice sheet	Geometry	$t = 2.0$ m; $L = 65$ m
	Intact ice	$E = 3500$ MPa; $c = 1.5$ MPa; $v = 0.35$; $\phi = 30^\circ$; $\sigma_T = 0.5$ MPa
	Failed ice	$E = 3500$ MPa; $c_r = 3.5$ Pa; $v = 0.35$; $\phi_r = 3^\circ$; $\sigma_{Tr} = 0.5$ Pa
	Viscoplastic properties	$\gamma = 1.0\ E-2$/sec; $N = 1$
Ice fragment	Fragmented ice	$\sigma_T = 0.5$ Pa; $\sigma_c = 1.5$ Pa; $\phi = 3^\circ$
	Inter-fragment interaction	$k_n^* = 1.0E$ 10 Pa; $c_i = 0$; $k_s^* = 1.0E$ 10 Pa; $\phi_i = 30^\circ$
Hydro-dynamic effects	Buoyancy and drag	$c_d = 1.0$; $(\rho_i/\rho_w) = 0.92$
Structure	Structural properties	$E = 2.0E$ 5 MPa; $\alpha = 0.32$; $v = 0.35$; $\beta = 0$; $\omega = 1.6$ Hz
	Structural geometry	$h = 20.0$ m; $h_1 = 15.0$ m; $b = 1.8$ m

response options include, (i) elastic behaviour in the intact state; (ii) viscoplastic behaviour predominantly in the compression range of the failure envelope which is characterized by the Mohr–Coulomb failure criterion; (iii) provision for fragment development in the tension and/or compression modes; and (iv) inter-fragment interaction responses which are characterized by an elastic–plastic response, the limiting values of which are governed by the Coulomb friction model. The values of the constitutive parameters are given in Table 1.

4.3. Interaction between the homogeneous ice sheet and flexible structure

We employ the discrete element procedure to examine the plane strain problem of the interaction of an ice sheet with the flexible structure. The basic objective of the analysis is to examine the influence of viscoplasticity phenomena and size dependency of the strength on the mode of fragmentation and on the development of the average contact stresses at the ice–structure interface.

Example 1:

This example deals with the problem of the plane strain dynamic interaction between the flexible cantilever structure and 2 m thick moving ice sheet with a prescribed far field velocity of 0.1 m/sec (Fig. 3). Both four-noded quadrilateral and three-noded triangular solid two-dimensional plane elements are used to model the viscoplastic ice sheet. The intact ice is assumed to have homogeneous constitutive properties (i.e. constant over the region of the ice sheet) at the start of the interaction process. In the constitutive modelling of the ice sheet, elastic behaviour is assumed in the intact state and the ice is assumed to experience fragmentation without viscoplastic flow in both the tensile and compressive states. It is assumed that after fragmentation, the ice exhibits a size dependent strength response as described previously. The strength characteristics of ice fragments can thus increase significantly after development of fragmentation as smaller size fragments are generated as a result of the interaction process. Figure 4 shows the initial mesh configuration in

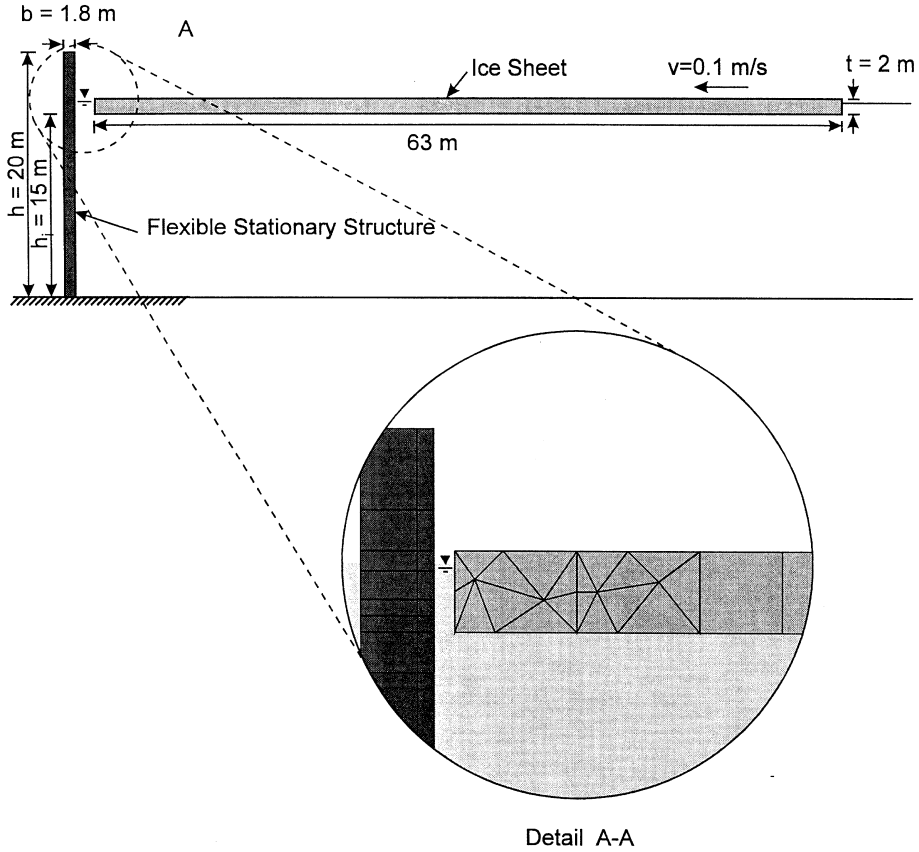

Fig. 3. Configuration of the ice–structure interaction problem.

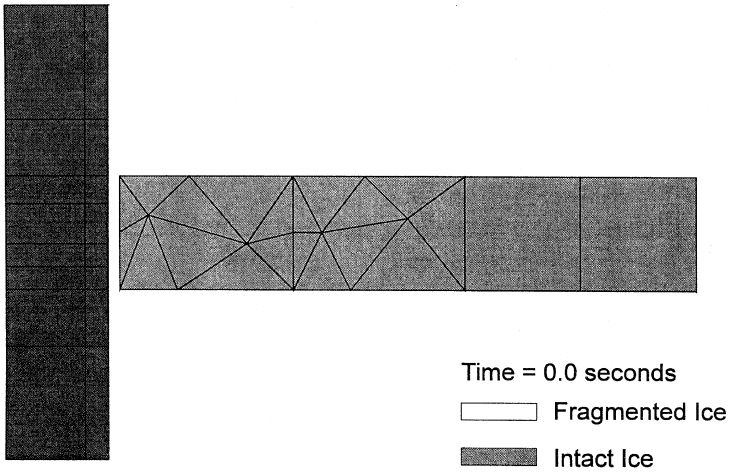

Fig. 4. Initial mesh configuration.

the vicinity of the ice–structure contact zone. A gap of 0.2 m between the ice sheet and the structure is assumed prior to the commencement of the computation process in order to simulate the impact between the ice sheet and the flexible structure. To minimize the computational effort, the 5 m section of the leading edge of the ice sheet which comes into contact with the structure is represented by discrete elements with elastic brittle fragmentation behaviour governed by the brittle fragmentation criteria. The region of the ice sheet beyond the 5 m section is modelled by elastic elements without provision for fragmentation. Self weight, buoyancy and drag forces on the ice are also included in the final computational modelling. Figure 5 illustrates the process of fragment development and fragmentation of the ice sheet in the vicinity of the flexible structure. As can be observed, interaction between the ice sheet and the structure occurs 2 s after the commencement of the movement. Fragmentation of the ice sheet occurs in the vicinity of the flexible structure immediately upon interaction. Further fragmentation of the ice sheet continues due to the ice–structure interaction process. Due to the imposed size dependent fragmentation stress, the strength characteristics of the smaller individual ice fragments are comparatively higher. This minimizes unrestricted development of smaller fragment sizes which can result in the termination of the computational process, primarily due to the restrictions on the computational capabilities. Figure 5 also illustrates a process similar to 'pile up' of ice fragments during the interaction process and indicates the distribution of normal contact stresses at the ice–structure interface. This result indicates that the location of the local peak stress fluctuates both in magnitude and location, due to the progressive development of fragmentation at the leading edge of the ice sheet. Figure 6 illustrates the time history of the average contact stress at the ice–structure contact region; an initial peak average contact stress pulse of approximately 1.0 MPa is observed for this case. The maximum observed contact stress is achieved 9.5 s after the commencement of the interaction process, where the continuum nature of the ice sheet is maintained in the upper region of the ice sheet. Characteristic pressure peaks in the average contact stress are observed during the interaction process (Fig. 6) as a result of the interaction of ice fragments with the flexible structure. The time history of the average stress also indicates an increasing trend with the accumulation of rubble in the vicinity of the structure as fragments are moved by an intact advancing ice sheet.

Example 2:

The basic geometry of the ice sheet and the structure, the element discretization and the speed of approach of the ice sheet, are identical to those used in Example 1. In this example, however, the constitutive behaviour of the ice sheet is changed to include elastic behaviour in the intact state, brittle fragmentation only when one or both principal stresses are in the tension range and viscoplastic failure when both principal stresses are in compression range. Figure 7 illustrates the pattern of fragment evolution during the dynamic contact between the ice sheet and the flexible structure. They also illustrate the distribution of normal contact stresses at the ice–structure interface. Figure 8 illustrates the time history of the average contact stresses at the ice–structure contact region; an initial peak average contact stress of approximately 7.40 MPa is observed. The maximum observed contact stress is achieved 4.0 s after the commencement of the interaction process. Similar to Example 1, the average contact stress history also indicates an increasing trend with the accumulation of rubble in the vicinity of the structure.

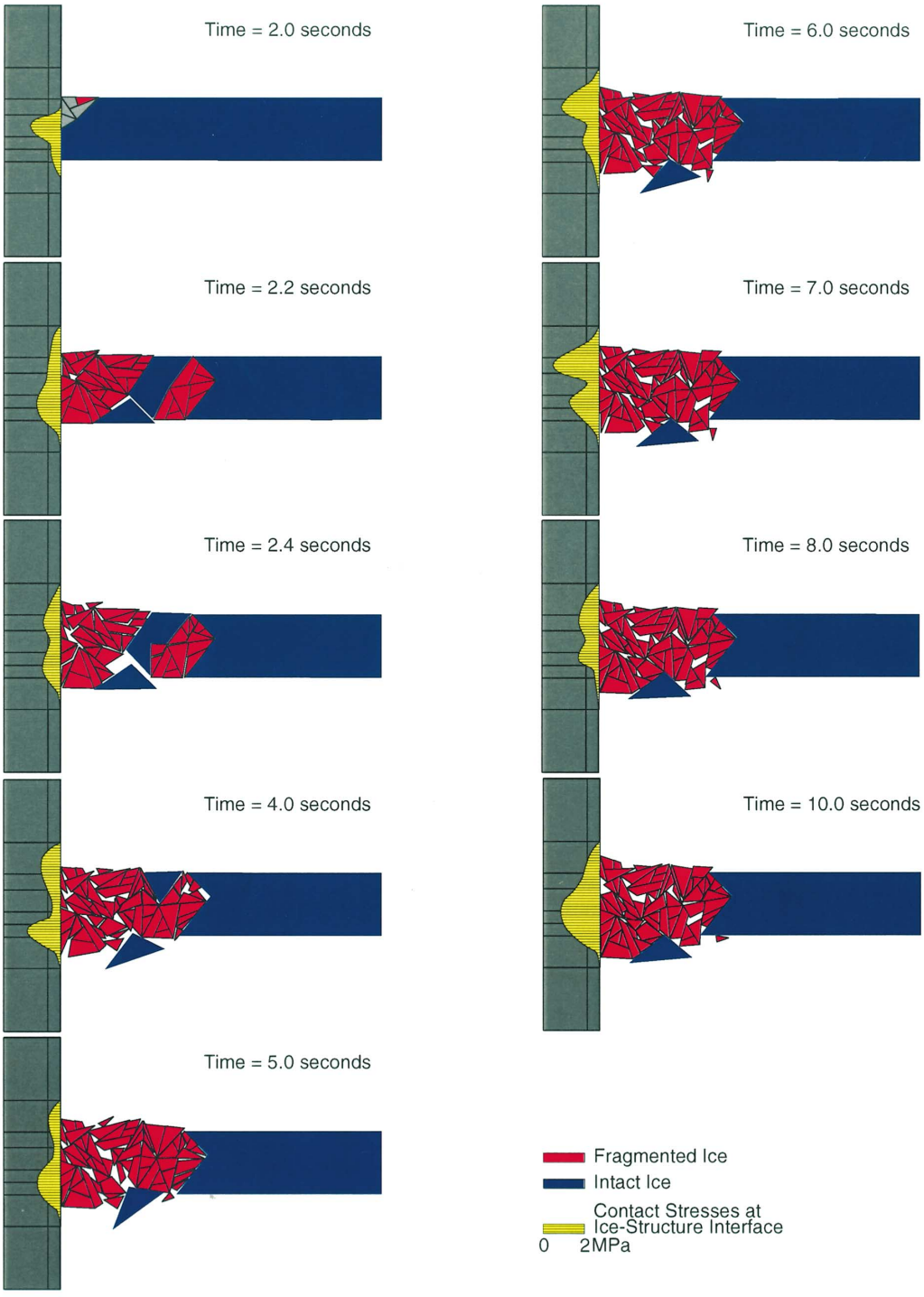

Fig. 5. Fragmentation of the ice sheet during the interaction process.

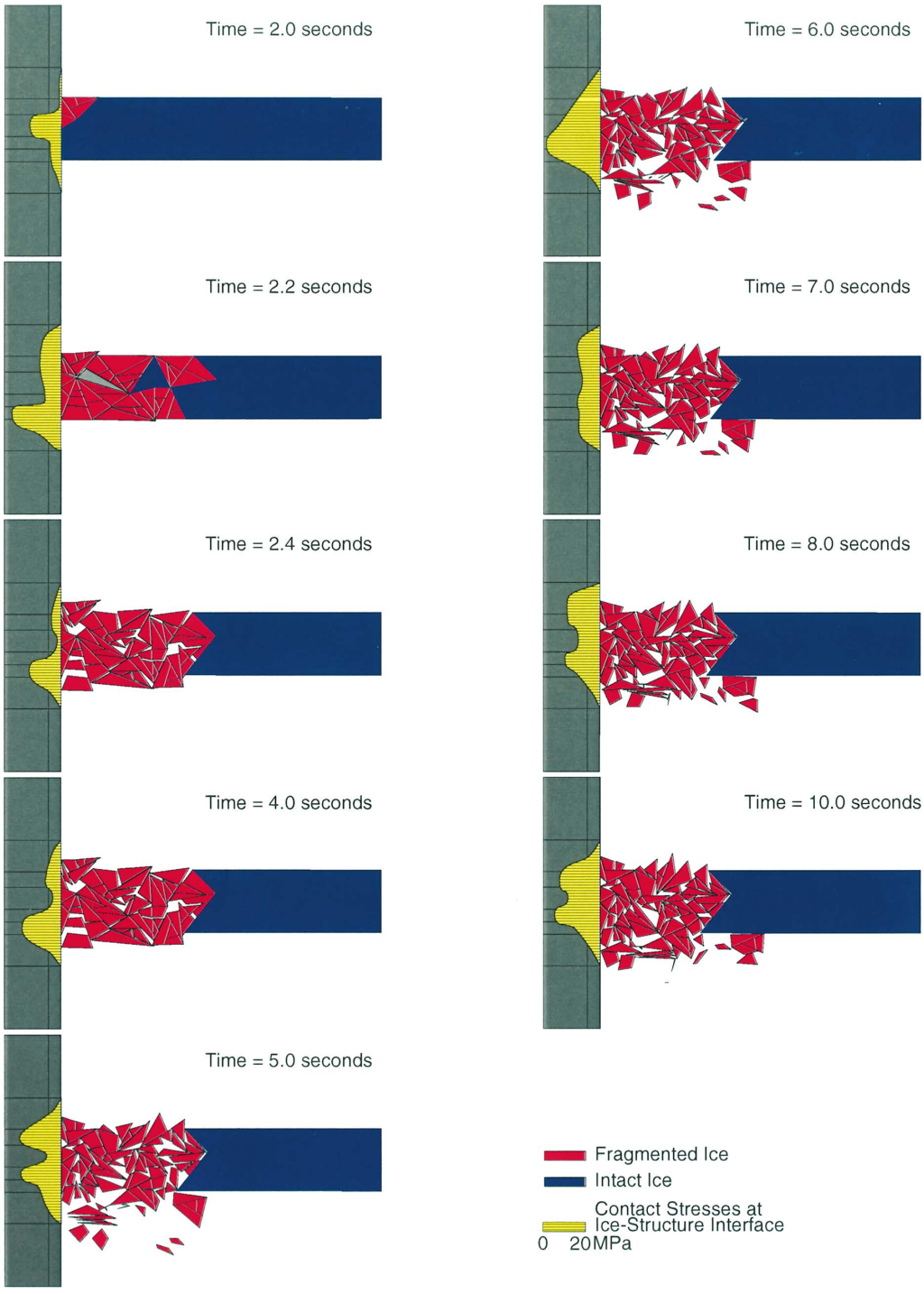

Fig. 7. Fragmentation of the ice sheet during the interaction process.

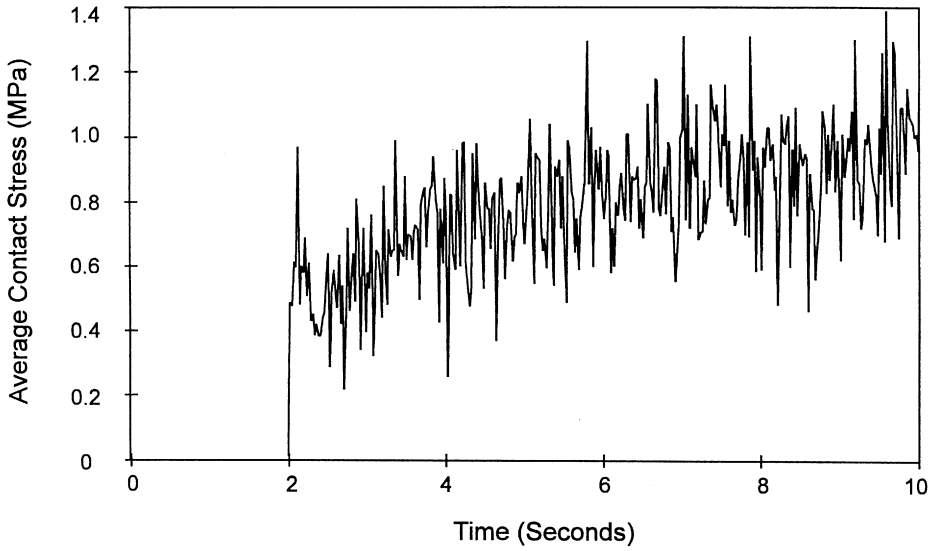

Fig. 6. Time-dependent variation of the average contact stress at the ice–structure interface.

5. Concluding remarks

This paper presents the results of a two-dimensional computational modelling exercise in the use of discrete elements for the study of an ice–structure interaction problem. The two aspects that have been investigated include, the utilization of the same failure criteria for describing both the initiation of viscoplastic flow in compression range and fragmentation in the tensile range and the inclusion of size dependency in the strength characteristics of the fragments that are produced during the interaction process. The first modification is incorporated to support the experimental observations which suggest that the processes of brittle fragmentation would occur in regions where the stress state is predominantly tensile and viscoplastic flow would occur in regions where the state of stress is predominantly compressive. The second modification is incorporated to limit the size of fragments developed during the interaction process which significantly influences the computational efficiency and the stability of the solution process. The size dependent strength criteria, particularly in relation to the tensile strength, is a realistic observation which is borne out by a variety of naturally occurring geomaterials. Consequently, the size dependency in the strength characteristics is viewed as a novel development which not only assists the computational efficiency of the solution scheme but also accounts for a realistic representation of brittle geomaterials, such as ice.

The modified discrete element code has been applied to examine the dynamic interaction between an ice sheet of constant thickness moving at a uniform speed with a stationary flexible structure. The first problem deals with an interacting ice sheet where a leading region of the ice sheet posses initial elastic characteristics and brittle fragmentation behaviour both in tension and compression. The remaining length is modelled as a non-fragmentable elastic layer. The fragmentation process illustrates the capabilities of a discrete element approach with the modifications discussed, to realistically duplicate the fragmentation process, limited only by a strength dependent fragment

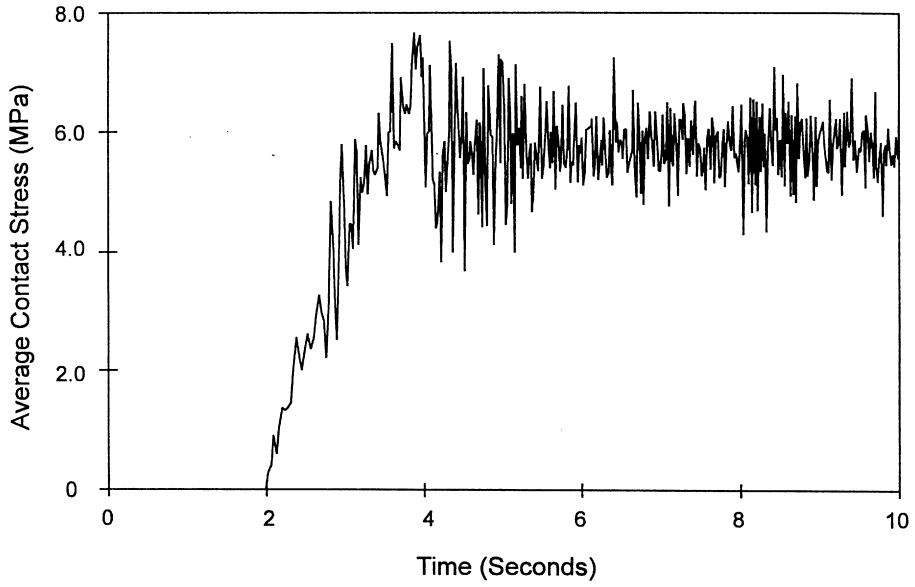

Fig. 8. Time-dependent variation of the average contact stress at the ice–structure interface.

size with a lowest edge length of 0.2 m. The time-dependent evolution of average contact stress exhibits the characteristic 'load accumulation–load shedding' feature observed during many ice–structure interaction phenomena. The periodicity of the process derived from this simulation is non-regular. This could be attributed to the highly irregular mesh configuration used to model the initial state of the ice sheet. A further observation of this study is the trend towards an increase in the average contact stress with penetration of the ice sheet, which indicates a possible influence of the ice rubble pile accumulation in the vicinity of the contact region. The fragment accumulation process shows evidence of the influence of gravity forces and buoyancy effects.

The second problem examined was similar in character except that only the leading ice sheet was modelled by a fragmentable, viscoplastic material. Viscoplastic flow occurs when principal stresses are both in the compressive mode and tensile fragmentation is assumed to occur only when at least one of the principal stresses is in the tensile mode. The time history of the average stresses indicates that the peak average stresses are induced within a relatively short duration of the interaction process. Similar to the previous example, the time-dependent evolution of average contact stress exhibits the characteristic 'load accumulation–load shedding' feature observed during interaction of ice sheets with offshore structures. Higher average contact stresses are, however, observed for this example as the ice sheet behaves as a region which can sustain stresses without shedding such loads by a fragmentation process.

Acknowledgements

The work reported in this paper was developed in connection with a National Energy Board of Canada (NEB) Research Project into Ice–Structure Interaction. The authors are grateful to Dr I.

Konuk formerly of the NEB for his continued support of the work and for the resources required to modify the DECICE code produced by INTERA (1986).

References

Bieniawski, Z.T., 1968. The effect of specimen size on compressive strength of coal. Int. J. Rock Mech. Mining Sci. 5, 325–335.

Blanchet, D., 1988. Variation of the load-failure pressure with depth through first year and multi year ice. Journal of Offshore Mech. and Arctic Engineering 110, 159–168.

Buck, E.B., Nickolyev, O.Y., Schulson, E.M., 1994. Failure envelopes and the ductile to brittle transition in S2 columnar fresh water and saline ice under biaxial compression. Proc. IAHR. Trondheim, Norway.

Comfort, G., Selvadurai, A.P.S., Abdelnour, R., Au, M.C., 1992. A numerical ice load model. Proc. Int. Assoc. Hydraulic Research Conf. Banff, Alberta, pp. 243–257.

Cormeau, I.C., 1975. Numerical instability in quasi-static elasto/visco-plasticity. Int. J. Num. Meth. Engng 9, 109–127.

Croasdale, K., 1984. Sea ice mechanics: a general overview. Marine Technology Society Journal 18 (1).

Dykins, J.E., 1970. Ice Engineering Tensile Properties of Sea Ice Grown in a Confined System. NCEL Technical Report R680.

Eranti, E., 1992. Dynamic Ice–Structure Interaction. VTT Tech. Research Centre of Finland, Espoo, Publication No. 90.

Eranti, E., Haynes, F.D., Häättänen, M., Soong, T.T., 1981. Dynamic ice–structure interaction analysis for narrow vertical structures. Proc. 6th Int. Conf. on Port and Ocean Engineering under Arctic Conditions (POAC), vol. 1. Quebec, Canada, pp. 472–479.

Fleet Technology Limited, 1996. Private Communication.

Frederking, R., 1993. Effects of scale on the indentation resistance of ice. POAC, vol. 1. Hamburg, pp. 37–48.

Goodman, R.E., 1980. Introduction to Rock Mechanics. John Wiley and Sons, p. 468.

Hallam, S.D., Pickering, J.G., 1988. Modelling of dynamic ice loading of offshore structures. Proc. POLARTECH, pp. 235–248.

Hobbs, D.W., 1967. Rock tensile failure and its relationship to a number of alternative measures of rock strength. Int. J. Rock Mech. Mining Sci. 4, 115–127.

Hocking, G., Mustoe, G.G.W., Williams, J.R., 1985a. Validation of the CICE code for the ice ride-up and ice ridge cone interaction. Civil Engineering in the Arctic Offshore, ASCE Specialty Conference. San Francisco, pp. 962–970.

Hocking, G., Williams, J.R., Mustoe, G.G.W., 1985b. Dynamic global forces on offshore structure from large ice flow impacts. Civil Engineering in the Arctic Offshore, ASCE Specialty Conference. San Francisco, pp. 202–219.

Hocking, G., Mustoe, G.G.W., Williams, J.R., 1987. Dynamic analysis for generalized three-dimensional contact and fracturing of multiple bodies. NUMETA 87, Swansea, U.K. A.A. Balkema, The Netherlands.

Ingraffea, A.R., 1987. Theory of crack initiation and propagation in rock, Chap. 3. In: Atkinson B.K. (Ed.), Fracture Mechanics of Rock. Academic Press, New York, pp. 71–110.

Ingraffea, A.R., Saouma, V., 1984. Numerical modelling of discrete crack propagation in reinforced and plain concrete, Chap. 4. In: Sih, G.C., de Tommaso, A. (Eds.), Applications of Fracture Mechanics to Concrete Structures. Martinus Nijhoff Publishers.

INTERA Technologies Inc., 1986. DEC-ICE Theoretical Manual. Lakewood, Colorado.

Jaeger, J.C., 1967. Failure of rocks under tensile conditions. Int. J. Rock Mech. Mining Sci. 4, 219–227.

Jaeger, J.C., Cook, N.G.W., 1976. Fundamentals of Rock Mechanics. John Wiley and Sons, p. 585.

Jahns, H., 1966. Measuring the strength of rock in situ at increasing scale. Proc. 1st Cong. ISRM (Lisbon) 1, 477–482.

Jefferies, M., Wright, W., 1988. Dynamic response of Molikpaq to ice–structure interaction. Proc. of the 7th Int. Conf. on Offshore Mechanics and Arctic Engineering, vol. IV. OMAE, pp. 201–220.

Jellinek, H.H.G., 1958. The influence of imperfections on the strength of ice. Proc. Physical Society of London 71, 797–814.

Joensuu, A., Riska, K., 1989. Ice and Structure Interaction. Helsinki University of Technology, Ship Laboratory. Report M-88, Espoo, Finland, p. 57.

Jordaan, I., McKenna, R., 1989. Modelling of progressive damage in ice. In. Timco, G. (Ed.), Working Group on Ice Forces, 4th State of the Art Report. CRREL Special Report 89-5.

Jordaan, I., Xiao, J., 1992. Interplay between damage and fracture in ice–structure interaction. Proc. International Association of Hydraulics Research (IAHR) Conference, vol. 3. Banff, Alberta, pp. 1448–1467.

Karr, D.G., Choi, C., 1989. A three-dimensional constitutive damage model for polycrystalline ice. Mechanics of Materials 8, 55–56.

Matlock, H., Dawkins, W.P., Panak, J.J., 1971. Analytical model for ice–structure interaction. Journal of Engineering Mechanics, ASCE EM4, 1083–1092.

Mulmule, S.V., Dempsey, J.P., Adamson, R.M., 1995. Large-scale in situ fracture experiments—Part II: modelling aspects. The American Society of Mechanical Engineers AMD 207, 129–146.

Mustoe, G.G.W., Williams, J.R., Hocking, G., Worgan, K., 1987. Penetration and fracturing of brittle plates under dynamic impact. NUMETA 87, Swansea, U.K. A.A. Balkema, The Netherlands.

Nadreau, J.P., Michel, B., 1986. Yield and failure envelope for ice under multiaxial compressive stresses. Cold Regions Science and Technology 13, 75–82.

Nixon, W.A., Kruger, A., Brown, T.G., 1994. Chaotic dynamic ice behaviour in Molikpaq ice–structure interactions. IAHR Ice Symposium, vol. 2. Trondheim, Norway, pp. 797–806.

Owen, D.R.J., Hinton, E., 1980. Finite Elements in Plasticity: Theory and Practice. Pineridge Press Ltd., Swansea, U.K.

Perzyna, P., 1966. Fundamental problems in viscoplasticity. In: Recent Advances in Applied Mechanics. Academic Press, New York.

Pratt, H.R., Black, A.D., Brown, W.D., Brace, W.F., 1972. The effect of specimen size on the mechanical properties of unjointed diorite. Int. J. Rock Mech. Mining Sci. 9, 513–530.

Richter-Menge, J., Claffey, M.J., 1991. Preliminary results of direct tension tests on first-year sea ice samples. In. Cold Regions Engineering, Proc. Sixth International Specialty Conference, ASCE. Hanover, NH, pp. 569–578.

Sanderson, T.J.O., 1988. Risks to Offshore Structures. Graham and Trotman, London.

Selvadurai, A.P.S., 1995. Boundary element modelling of geomaterial interfaces. In: Selvadurai, A.P.S., Boulon, M.J. (Eds.), Mechanics of Geomaterial Interfaces, Studies in Applied Mechanics, vol. 42. Elsevier Scientific Publishers, pp. 173–197.

Selvadurai, A.P.S., Au, M.C., 1992. Damage and viscoplasticity effects in the indentation of a polycrystalline solid, In: Boehler, J.P., Khan, A.S. (Eds.), Plasticity '91, Proceedings 3rd International Symposium on Plasticity and its Current Applications. Elsevier Science Publishers, Grenoble, The Netherlands, pp. 405–408.

Selvadurai, A.P.S., Boulon, M.J. (Eds.), 1995. Mechanics of Geomaterials Interfaces, Studies in Applied Mechanics, vol. 42. Elsevier Science Publishers, The Netherlands, p. 553.

Selvadurai, A.P.S., ten Busschen, A., 1995. Mechanics of the segmentation of an embedded fibre—Part II: computational modelling and comparison. J. Appl. Mech. ASME 62, 98–107.

Selvadurai, A.P.S., Sepehr, K., 1995. On the indentation of a blunt ice wedge. ISOPE-95, vol. II. The Hague, The Netherlands, pp. 317 –322.

Selvadurai, A.P.S., ten Busschen, A., Ernst, L.J., 1993. Computational models for fragmentation tests. In: Dijksman, J.F., Nieuwstadt, F.T.M. (Eds.), Integration of Theory and Applications in Applied Mechanics, 2nd National Mechanics Congress in the Netherlands, Topics in Applied Mechanics. Kluwer Academic Publishers, Rolduc, The Netherlands, pp. 97–110.

Sodhi, D.S., Nakazawa, N., 1990. Frequency of intermittent ice crushing during indentation tests. Proc. 10th Int. Assoc. of Hydraulics Research (IAHR) Symposium on Ice, vol. 3. Espoo, Finland, pp. 277–289.

Timco, G.W., Frederking, R.M.W., 1984. An investigation of the failure envelope of granular/discontinuous columnar sea ice. Cold Regions Science and Technology 9, 17–27.

Williams, J.R., Mustoe, G.G.W., Worgan, K., 1986. Force transfer and behaviour of rubble piles. Proc. IAHR Ice Symposium, vol. 1. Iowa City, IO, pp. 615–626.

Zienkiewicz, O.C., Cormeau, I.C., 1974. Viscoplasticity, plasticity and creep in elastic solids—a unified numerical solution approach. Int. J. Numerical and Analytical Methods in Engineering 8, 821–845.